Accurate deployable mirrors for small optical CubeSat telescope: design and laboratory validations

Katherine Morris, Noah Schwartz, Zeshan Ali, Maria Milanova, Chris Miller, Junyi Zhou, David Isherwood, William Brzozowski, Rory Gillespie, Charlotte Bond, Douglas Harvey, Lawrence Bissell, Éamonn Harvey, Jay Stephan, Amelia Calderhead, Raziye Artan, Amna Waris, Stella Gouzon, Cassandra Mercury

Published version information:

Citation: Katherine Morris et al., Accurate deployable mirrors for small optical CubeSat telescope: design and laboratory validations, Proceedings Volume 13092, Space Telescopes and Instrumentation 2024: Optical, Infrared, and Millimeter Wave; 130922T (2024)

DOI: https://doi.org/10.1117/12.3020184

Accurate deployable mirrors for small optical CubeSat telescope: design and laboratory validations

Katherine Morris[a], Noah Schwartz[a], Zeshan Ali[a], Maria Milanova[b], Chris Miller[a], Junyi Zhou[a], David Isherwood[a], William Brzozowski[a], Rory Gillespie[a], Charlotte Bond[a], Douglas Harvey[a], Éamonn Harvey[a], Jay Stephan[a], Amelia Calderhead[a], Raziye Artan[a], Amna Waris[a], Stella Gouzon[a], and Cassandra Mercury[a]

[a]UK Astronomy Technology Centre, Blackford Hill, Edinburgh, United Kingdom
[b]University of Bern, Bern, Switzerland

ABSTRACT

A-DOT (Active Deployable Optical Telescope) is a payload prototype of a 6U deployable telescope operating in the visible from 400 to 800 nm with an aperture diameter of 300 mm. It aims to deliver diffraction-limited performance using on-board wavefront sensing (WFS) and active control (WFC). A-DOT is currently in the design phase.

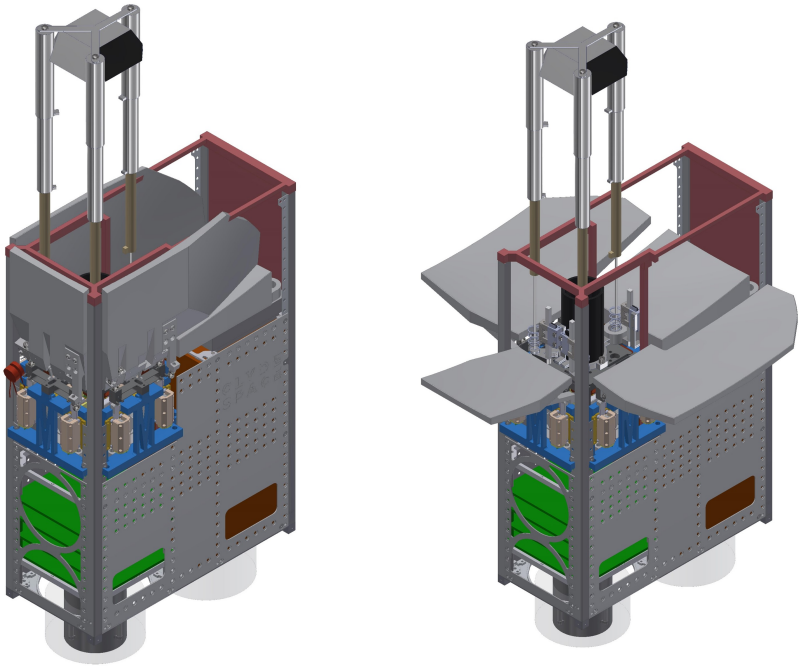

Figure 1: A-DOT CubeSat assembly in stowed and deployed configuration

This paper presents the development of a deployable, single-segment, mechanical prototype. The deployable mirror segment is kinematically mounted to a monolithic flexure using three spherical contacts in a cup-groove-flat arrangement. Tip, tilt and piston (PTT) are controlled using linear, piezoelectric actuators at each contact and the mirror position measured using capacitive sensors. The prototype is packaged within the allowable CubeSat volume and uses space-compatible hardware in a non-magnetic design.

Keywords: Telescope, Mirror, Deployable, Actuator, CubeSat

Further author information:
Katherine Morris: E-mail: katherine.morris@stfc.ac.uk

Space Telescopes and Instrumentation 2024: Optical, Infrared, and Millimeter Wave, edited by Laura E. Coyle, Shuji Matsuura, Marshall D. Perrin, Proc. of SPIE Vol. 13092, 130922T · © 2024 SPIE · 0277-786X · doi: 10.1117/12.3020184

1. INTRODUCTION

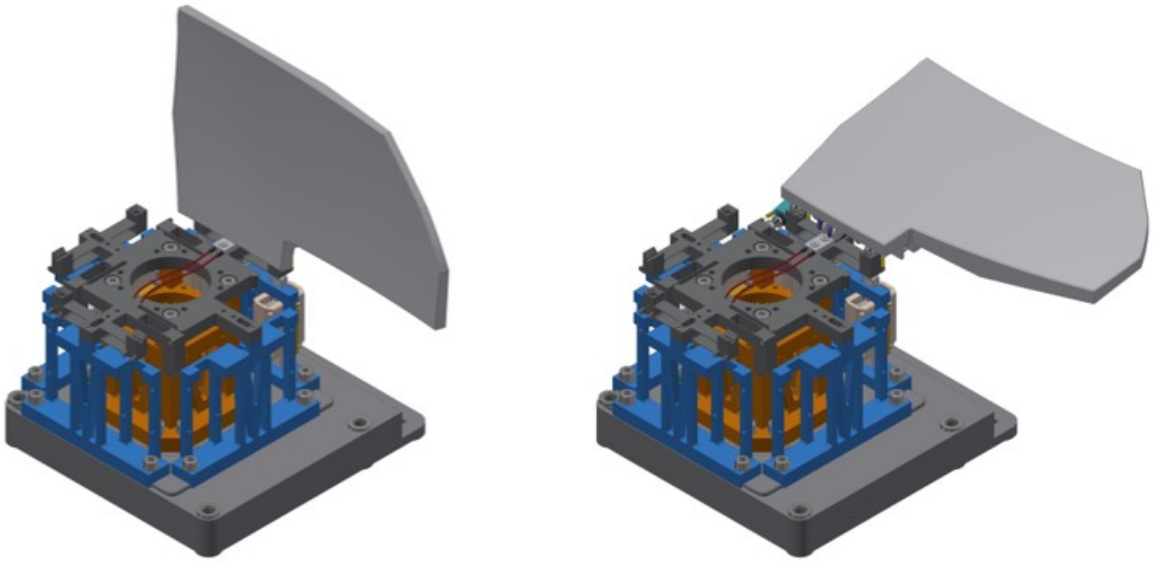

Figure 2: Mechanical M1 demonstrator in stowed and deployed configuration

The principal of M1 petal deployment has been conceptualised and successfully demonstrated in the four M1 petal, High-resolution deployable CubeSat [1]. A-DOT uses a floating hinge created by tooling balls within a cup-v-groove-flat kinematic mount and piezoelectric actuators to locate and co-phase the M1 petals to a continuous optical surface. To prove the feasibility of the mechanical design; particularly the actuation of larger deployable M1 petals, a mechanical laboratory demonstrator was developed. Figure 2 shows the demonstrator with a single petal in both stowed and deployed configurations.

2. DEMONSTRATOR DESIGN

The overall design for the single petal demonstrator was based upon the flight arrangement of three deployable petals, with each petal controlled by three actuators. The actuator module must be contained within a volume of approximately 1U (a 100x100x100 mm cube).

2.1 Actuator selection

Actuators were selected by obtaining the minimum required actuation force based on the uncertainty factors within the system to be actuated. The ECSS mechanisms standard [2], an applicable standard for in-orbit demonstration CubeSat projects developed through the ESA General Support Technology Programme activity entitled "CubeSat Technology Pre-Development", is employed to calculate minimum actuation forces. Minimum actuation force, F_{min}, is derived from equation:

$$F_{min} = 2(1.1I + 1.2S + 1.5H_M + 3F_R + 3H_Y + 3H_A + 3H_D) + 1.5F_D + F_L \quad (1)$$

Uncertainty symbols and associated factors are summarised in Table 1.

It was deemed that the resistive spring force and friction uncertainties were sufficient for calculating the minimum required actuator force, simplifying the equation to:

$$F_{min} = 2(1.2S + 3F_R) \quad (2)$$

Resistive orbital inertial forces were considered negligible and likely less than gravity forces. For ground based testing, the weight of the largest petal is around 5N. Employing the equation for minimum actuation force, F_{min}, and including a term for weight, the required actuation force at the cup and v-groove locations is around 37N. For actuation at the flat, 78N is calculated due to the moment created by the petal weight around the tooling ball axis. It was deemed that this significant increase in actuation force required for ground-based testing would result in significant oversizing of motors and make accommodation even more challenging. Therefore, a plan was created to employ a spring to reduce some of the moment created by the petal on the flat interface. The location of this is described further in Section 2.5. The PiezoLegs LT40 was considered the most suitable actuator, able to provide a force of 40 N. Previous testing using the LT20, a smaller version of this actuator had previously been tested with positive results.

Table 1: Minimum uncertainty factors for actuation function.

Resistive torque or force contributor	Symbol	Theoretical factor	Measured factor
Inertia	I	1.1	1.1
Spring	S	1.2	1.1
Magnetic effects	H_M	1.5	1.1
Friction	F_R	3	1.5
Hysteresis	H_Y	3	1.5
Others(e.g. Harness)	H_A	3	1.5
Adhesion	H_D	3	3

2.2 Actuator support structure and kinematic mount

Due to the geometry of the actuator, the monolithic kinematic mount was designed to have one interface normal to the others as shown in Figure 3.

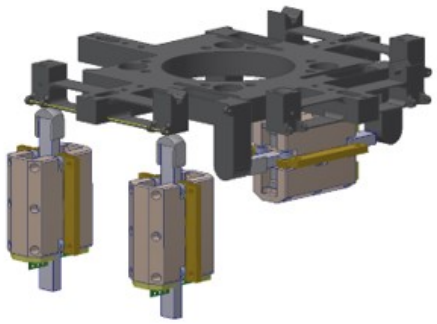

Figure 3: Kinematic mount and actuator arrangement

The demonstrator therefore used the same arrangement, allowing for all deployable petals and actuators to be integrated however, only one large petal was tested. From this arrangement, support structures were designed to mount the actuators while allowing their positions to be adjustable. The overall kinematic mount and actuator structure is shown in Figure 4. Included in this structure is the shape memory alloy used to dampen the M1 petal deployment as outlined in Ref [1]. The kinematic mount was made from Aluminium-6082-T6 as this provided the flexures with an appropriate stiffness and machinability. All other components in the support structure were made from Aluminium-6082-T6, to match this part.

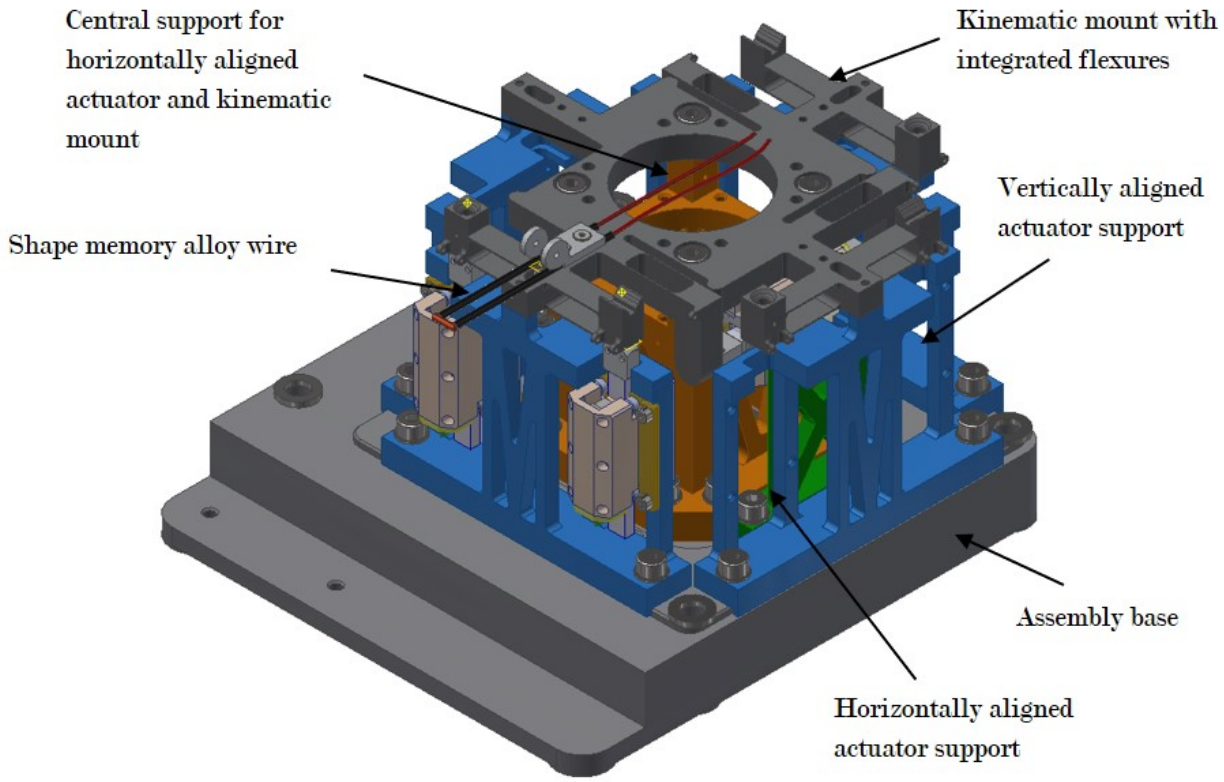

Figure 4: Kinematic mount and actuator support structure

2.3 M1 petal

The M1 petal assembly was designed with several integrated features to allow position adjustment, along with locations for attaching small springs to retain the spherical tooling ball contacts within the kinematic mount shown in Figure 5. The deployable petal was made from Aluminium-6061-T6 as this is considered appropriate for producing optical surfaces. The tooling ball arm and hinge with spring mounting points were made from Aluminium 6082-T6 similar to the support structure. The tooling ball mounting block and spacers were made from Stainless steel 1.4401 to match the mechanical properties of the COTS tooling balls.

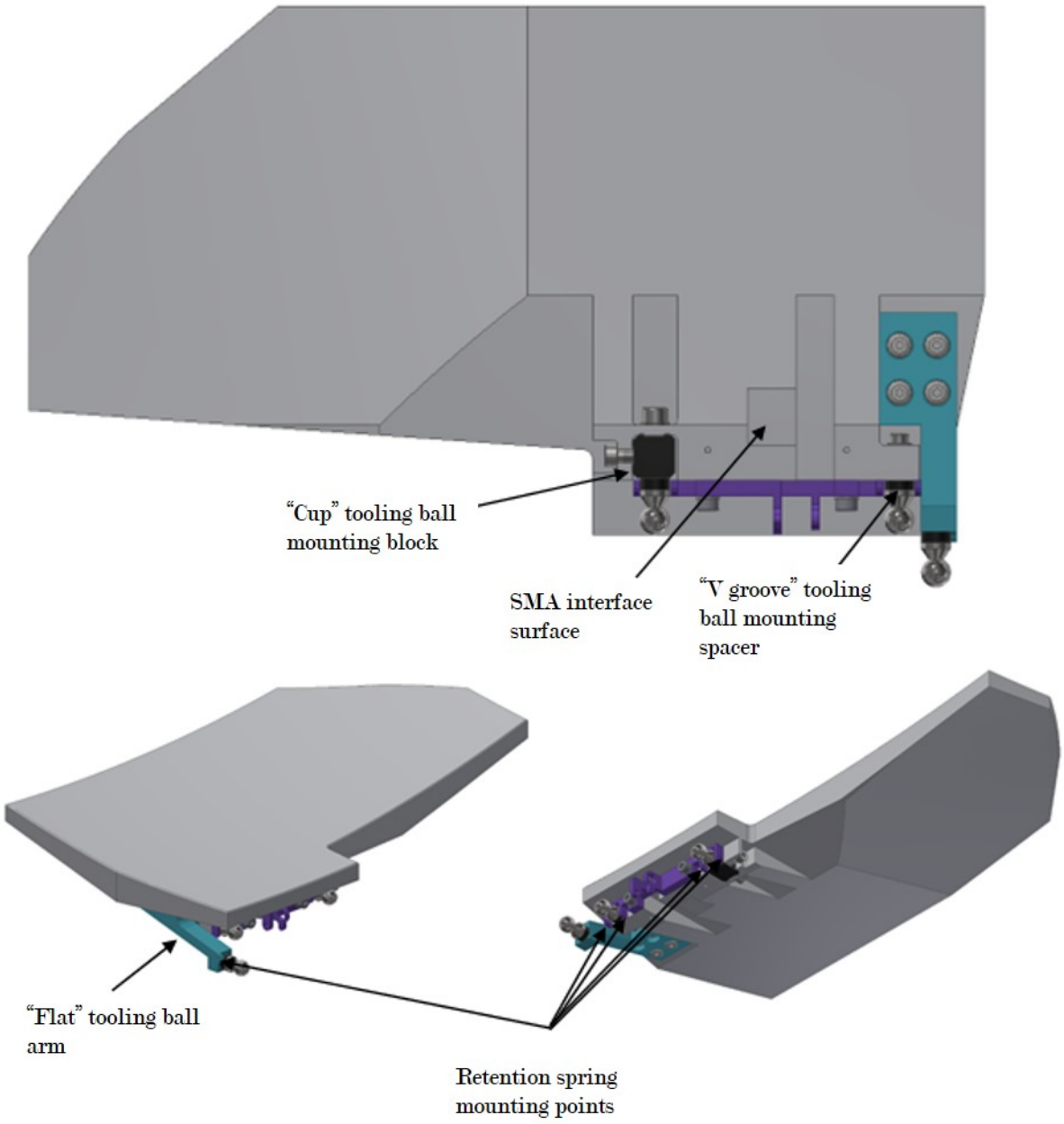

Figure 5: Deployable M1 petal integrated features

2.4 Capacitive sensors

The position of the demonstrator M1 petal was to be measured mechanically using MicroEpsilon CSE05 capacitive sensors. The petal therefore did not require an optical surface, but several interface surfaces were selected to measure using the sensors shown in Figure. The sensors are numbered to identify them in the results.

Figure 6: MicroEpsilon CSE05 capacitive sensor cluster

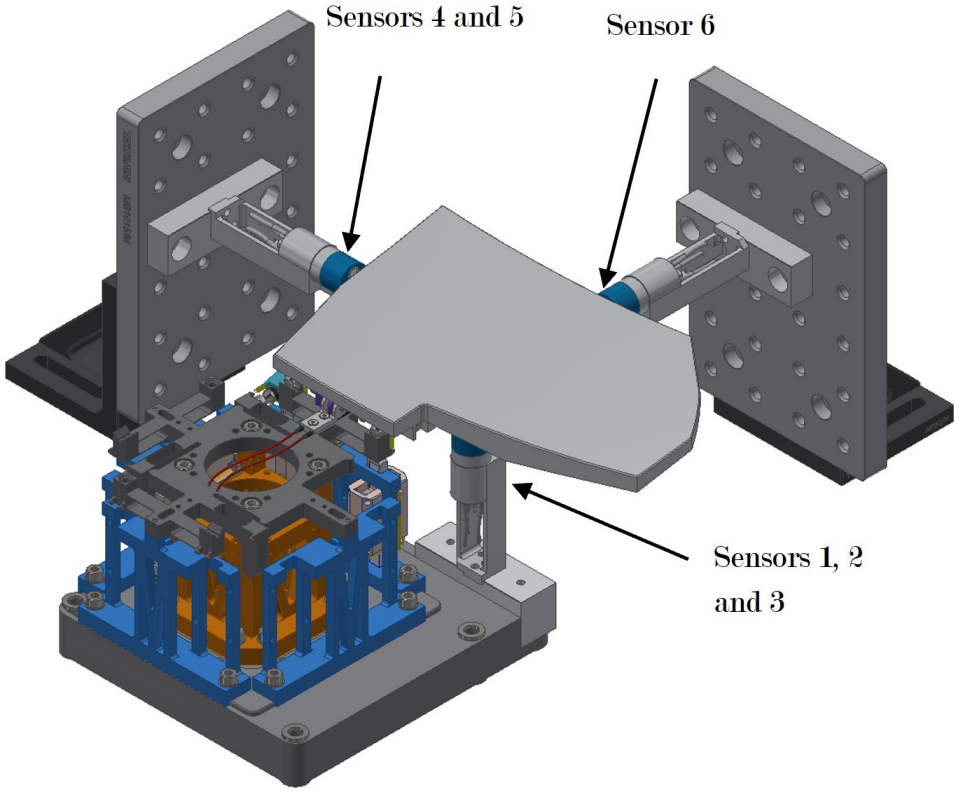

Figure 7: Sensor locations

2.5 Overall assembly

A large spring was included in the test assembly to reduce the moment created by the mass of the deployable petal on the "flat" kinematic mount interface. The location of this "anti-gravity" spring is shown in Figure 8.

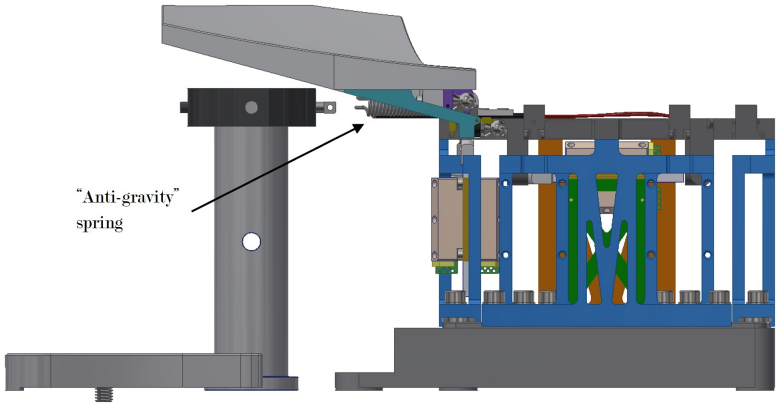

Figure 8: "Anti-gravity" spring location

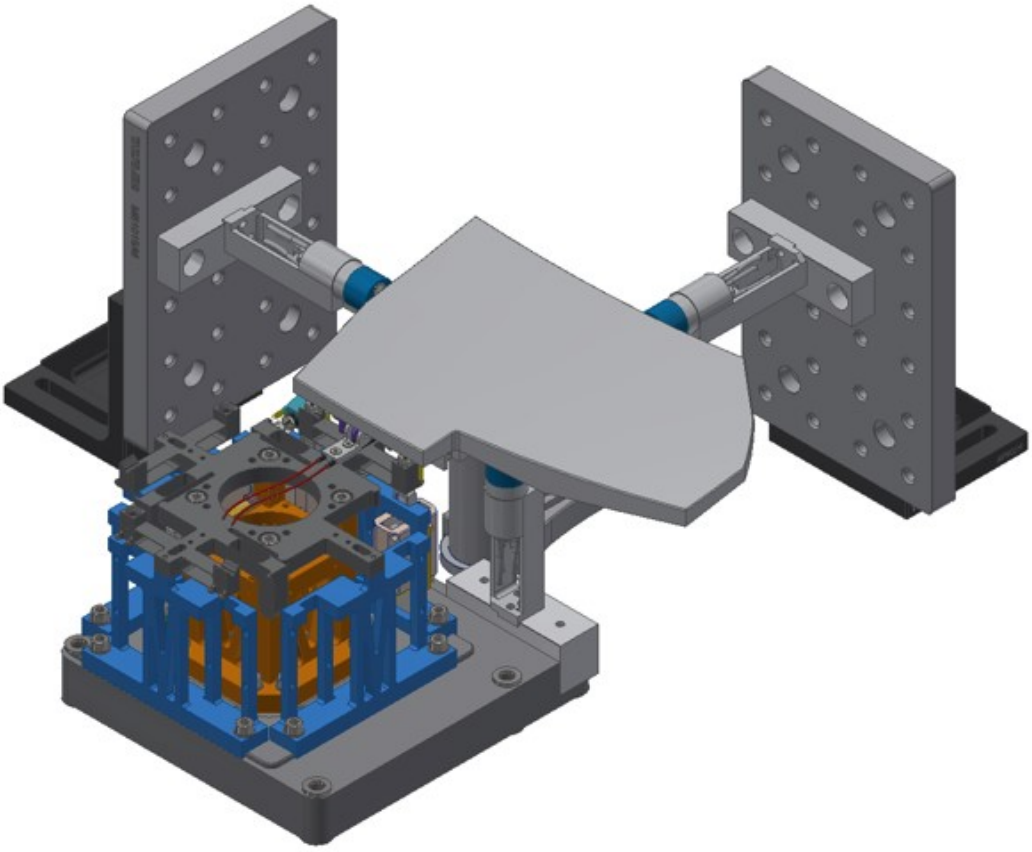

Figure 9: Demonstrator test assembly

3. DEMONSTRATOR ASSEMBLY

The demonstrator was assembled as shown in Figure 10. The anti-gravity spring was removed as it pulled the v-groove tooling ball out of the kinematic mount.

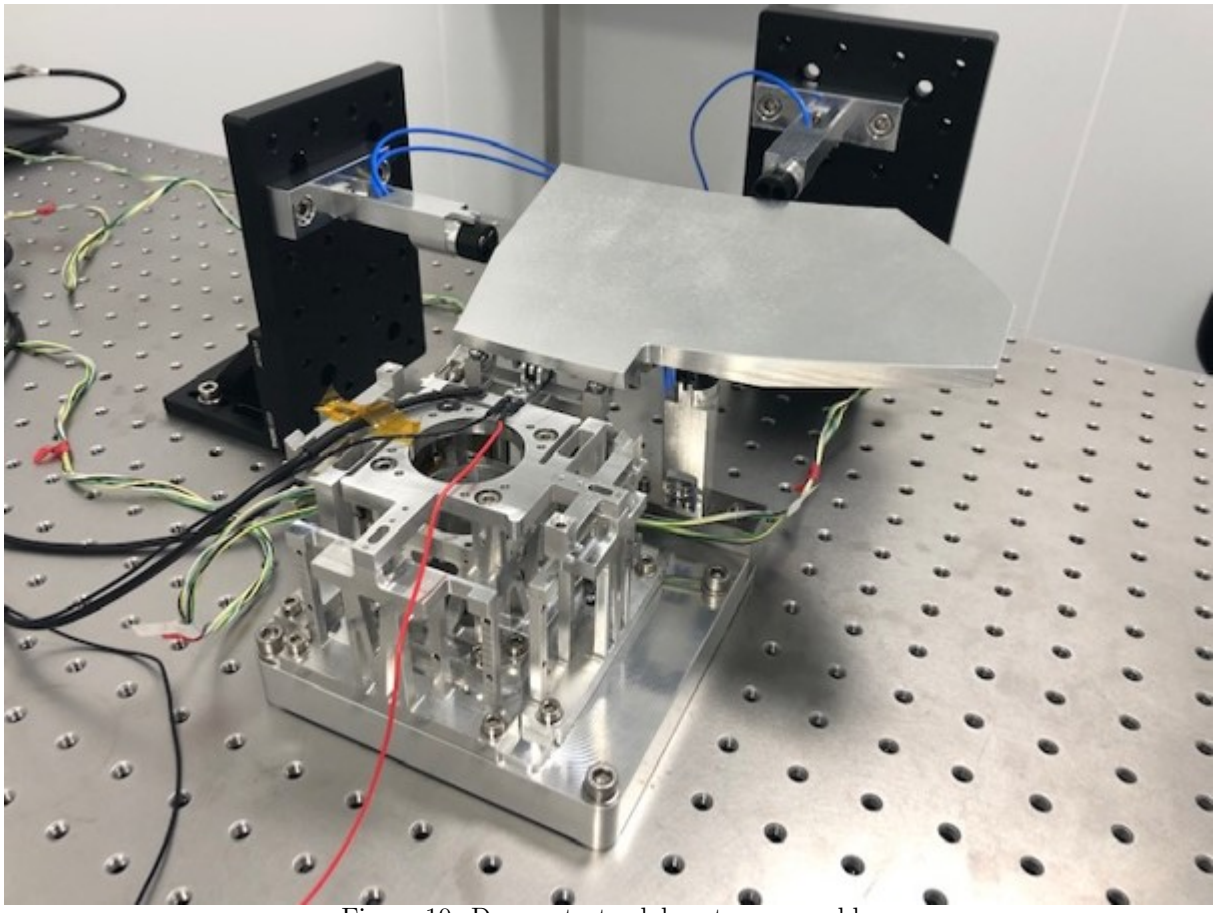

Figure 10: Demonstrator laboratory assembly

4. TESTING

To successfully apply the M1 co-phasing algorithm, the M1 optic petals must be deployed accurately and their positions controlled while in space. The key requirements for the CubeSat are:

- Accurate deployment of optics to ± 5 µm.
  - Deployment accuracy in piston is not as critical since the deployable petals can be actuated in this direction.
- Accurate control of optics to ± 10 nm.

A testing strategy was therefore created to assess how well the demonstrator would meet these requirements. The repeatability component of deployment accuracy must be measured. This was achieved by deploying the petal multiple times and recording its position using the array of capacitive sensors. To characterise the resolution and repeatability of the tip/tilt/piston actuation method, piezoelectric actuators were used to control the position of the three tooling balls. The petal location was measured using the array of capacitive sensors.

4.1 Deployment repeatability

Deployment repeatability was tested by retracting and deploying the petal into its kinematic mount 500 times. After each deployment, the petal was allowed to settle into position for 10 seconds. Position was measured using the vertically mounted cluster of three capacitive sensors. The experiment was then repeated and measurements taken using the horizontally mounted capacitive sensors. Preliminary testing had shown that sensor measurements were sensitive to environmental conditions. Temperature data was recorded concurrent to sensor measurements to identify any correlation between datasets. Removing a linear trend correlating to thermal drift gives the results shown in Figure 11 and Figure 12.

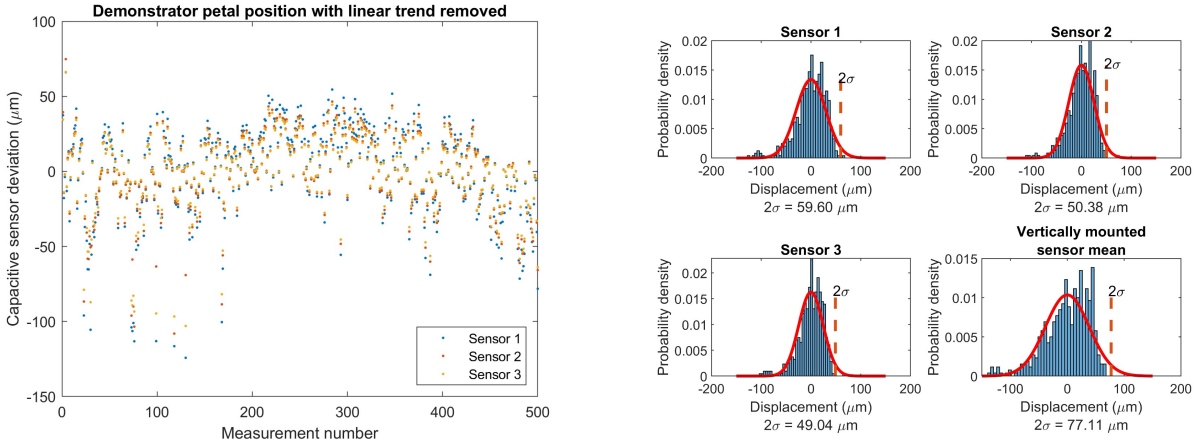

Figure 11: Measured displacement with thermal trend removed and distribution - vertically mounted sensors

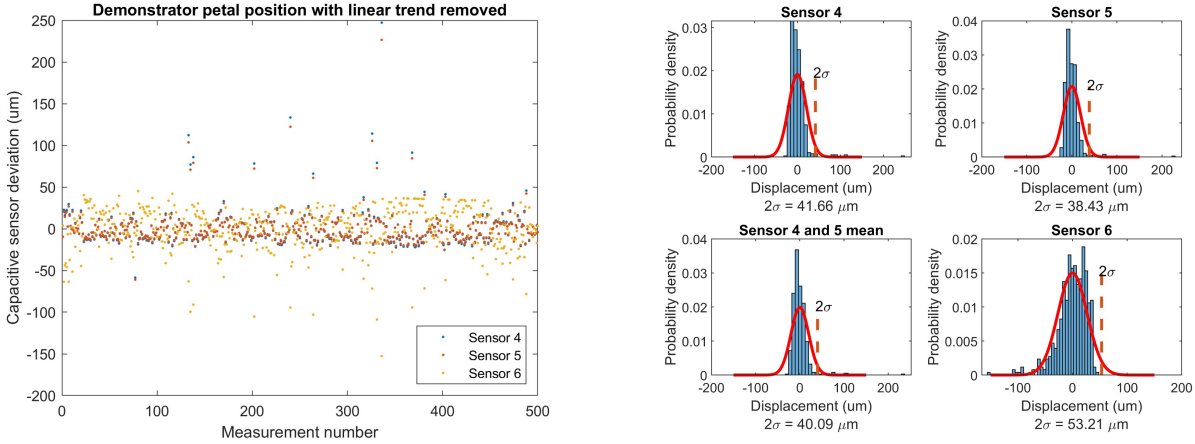

Figure 12: Measured displacement with thermal trend removed and distribution - horizontally mounted sensors

The distribution of the measurement data for each sensor, along with a mean for each sensor cluster is shown. The red line shows a normal distribution fit to the data. For each sensor, the 2σ variation (95% confidence) around the mean is outside the required tolerance of $\pm$ 5 µm. This can potentially be explained by the demonstrator geometry. A significant portion of the M1 petal is unsupported by the floating hinge; this mass creates a moment around the "cup" of the kinematic mount shown in Figure 13. While the retention springs were selected to theoretically counter this turning force, it was clear during testing that they were not in an optimal location to do so. The lack of the large "anti-gravity" spring to account for the mass of the petal also likely had a significant effect on the repeatability of the measurements.

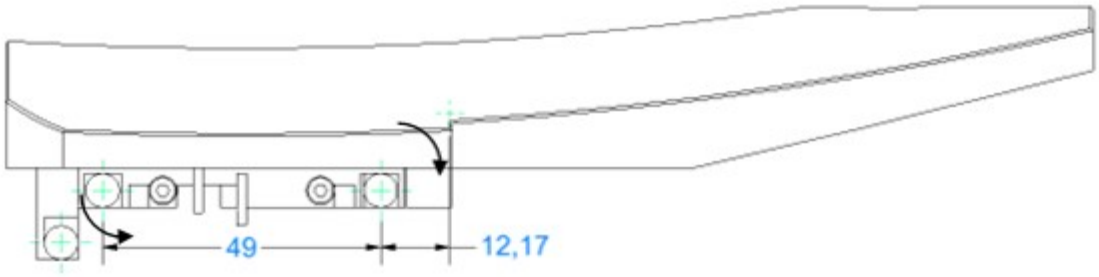

Figure 13: Moments around "cup" tooling ball

4.2 Alignment control

Driving either the "cup" or "v-groove" actuator provides tip, while the "flat" actuator provides tilt. Driving both the "cup" and "v-groove" actuators provides piston. Resolution and repeatability of the PTT actuation method was tested by driving each of the actuators to a set point using a user defined step size and measuring after each step using the sensor cluster. Each actuator was used to drive its kinematic mount flexure to a midpoint of 100 µm; allowing for forward and backwards movement. This can be considered as the "zero" or "null" point. The experiment was entirely automated, including actuation movement and measurement taking. Temperature was measured concurrent to displacement measurements, however, the plots are still to be produced and resultant detrending to be introduced where applicable.

4.2.1 "Cup" tooling ball tip

The "cup" actuator was driven from zero to 500 nm and back in steps of 1.6479 nm with a measurement taken after every movement. Measurements shown in Figure 14 describe the petal tip.

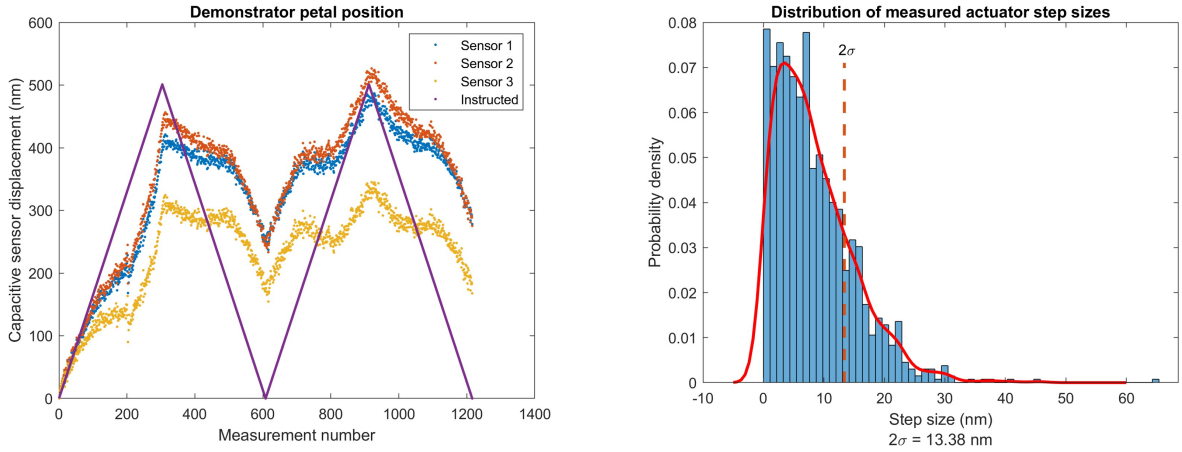

Figure 14: Measured displacement from tip and distribution

4.2.2 "V-groove" tooling ball tip

The experiment described in Section 4.2.1 was repeated using the "v-groove" actuator. Measurements shown in Figure 15 describe the petal tip.

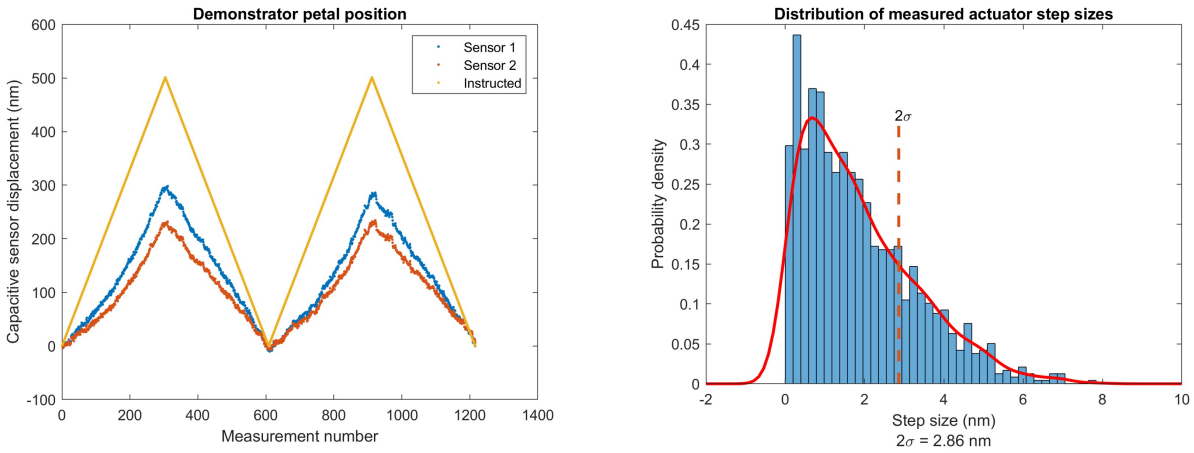

Figure 15: Measured displacement from tip and distribution

4.2.3 "Flat" tooling ball tilt

The experiment described in Section 4.2.1 was repeated using the "flat" actuator. Measurements shown in Figure 16 describe the petal tilt.

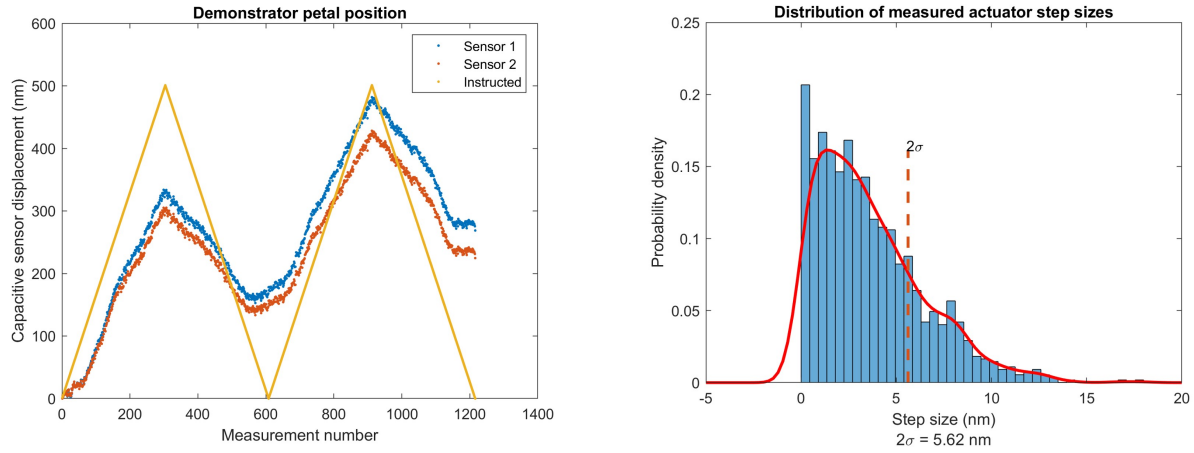

Figure 16: Measured displacement from tilt and distribution

The results from each of the experiments show that the open-loop step size is quite unpredictable, and that hysteresis causes uncertainty in the measured petal position. However, the step size distribution plots show that nanometre resolution of the linear actuators used to control alignment is achievable. Active optics using focal-plane wavefront sensing [3] to phase the mirror segments will likely improve the alignment.

5. CONCLUSION

A single-segment, deployable telescope mirror demonstrator was developed for A-DOT. The deployment repeatability of approximately 50 µm was measured however, several changes to the demonstrator are suggested to improve this: supporting petal mass, changing position of retention springs and reducing force on the "flat" kinematic mount. Though step size was unpredictable, nanometre resolution alignment was achieved using piezoelectric linear actuators and measured using capacitive sensors.

ACKNOWLEDGMENTS

This paper describes work that was performed within the Early-stage research and development scheme entitled "Active Deployable Optical Telescope". The United Kingdom Astronomy Technology Centre was awarded funding through the United Kingdom Science and Technology Facilities Council STFC (Grant no. ST/X004791/1).

References

[1] Schwartz, N., Brzozowski, W., Milanova, M., Morris, K., Todd, S., Ali, Z., Sauvage, J.-F., Ward, A., Lunney, D., and MacLeod, D., "High-resolution deployable CubeSat prototype," in [*Space Telescopes and Instrumentation 2020: Optical, Infrared, and Millimeter Wave*], Lystrup, M., Perrin, M. D., Batalha, N., Siegler, N., and Tong, E. C., eds., **11443**, 1144331, International Society for Optics and Photonics, SPIE (2020).

[2] European Cooperation for Space Standardization, "Space Engineering Mechanisms." ECSS Secretariat, ESA-ESTEC Requirements & Standards Division (2019).

[3] Schwartz, N., Harvey, E., Sanchez, S. P., Yeung, S.-L., Harvey, D., Stephan, J., Zhou, J., Morris, K., and Bond, C., "Phasing a small deployable optical space telescope using focal-plane wavefront sensing," in [*Astronomical Telescopes and Instrumentation 2024: Wavefront Sensing and Segment Phasing*], SPIE (2024).